Received: 1 September 2018 | Revised: 23 December 2018 | Accepted: 16 February 2019

DOI: 10.1002/asl.890

Atmospheric Science Letters RMetS

RESEARCH ARTICLE

Interdecadal changes in potential predictability of the summer monsoon in East Asia and South Asia

Baosheng Li[1,2,3] | Ruiqiang Ding[2,3] | Jianhuang Qin[1] | Lei Zhou[1,2] | Shuai Hu[3] | Jianping Li[2,4]

[1]Institute of Oceanography, Shanghai Jiao Tong University, Shanghai, China

[2]Laboratory for Regional Oceanography and Numerical Modeling, Qingdao National Laboratory for Marine Science and Technology, Qingdao, China

[3]State Key Laboratory of Numerical Modeling for Atmospheric Sciences and Geophysical Fluid Dynamics (LASG), Institute of Atmospheric Physics, Chinese Academy of Sciences, Beijing, China

[4]College of Global Change and Earth System Sciences (GCESS), Beijing Normal University, Beijing, China

Correspondence
Ruiqiang Ding, Institute of Atmospheric Physics (IAP), Chinese Academy of Sciences (CAS), No.40, Huayanli, Chaoyang District, Beijing, 100029, China.
Email: drq@mail.iap.ac.cn

Funding information
National Key Technology Research and Development Program of the Ministry of Science and Technology of China, Grant/Award Number: 2015BAC03B07; National Program on Global Change and Air-Sea Interaction, Grant/Award Numbers: GASI-IPOVAI-03, GASI-IPOVAI-06; the 973 project of China, Grant/Award Number: 2016YFA0601801

Interdecadal changes in the potential predictability of the East Asian summer monsoon (EASM) and South Asian summer monsoon (SASM) were investigated using the signal-to-noise ratio of daily reanalysis data from 1948 to 2017. Results reveal that variations in the SASM predictability are out of phase with those in EASM predictability, and that SASM predictability is higher (lower) than EASM predictability before (after) the 1980s. The out-of-phase relationship of the predictability of the two monsoon systems is attributed mainly to temporal changes in their relationships with El Niño-Southern Oscillation (ENSO). The relationship between the EASM and ENSO is related to the position of the ENSO heating center, which is located in the central Pacific before the 1980s but shifted to the eastern Pacific after the 1980s, accompanied by a strengthening (weakening) in the relationship between ENSO and the EASM (SASM). The shift in the position of the ENSO heating center was found to have contributions from the modulation of the Pacific decadal oscillation.

KEYWORDS

East Asian summer monsoon (EASM), ENSO, South Asian summer monsoon (SASM), predictability

1 | INTRODUCTION

The East Asian summer monsoon (EASM) and the South Asian summer monsoon (SASM) are two major components of the Asian monsoon system, which itself is part of the global monsoon system, and they play an important role in modulating precipitation and wind fields, which have important effects on climate change in Asia (Lau and Weng, 2001; Ding and Chan, 2005; Chang *et al.,* 2011). Thus, accurate predictions of the summer monsoon are vital to obtaining reliable forecasts of intense precipitation and associated flood events across East Asia (Webster *et al.,* 1998; Wu *et al.,* 2006, 2009). As predictability is an inherent nature of the monsoon system (Li and Chou, 1997), a comparison of the predictability of these two monsoon systems will benefit efforts to improve monsoon and related precipitation forecasts.

To explore the monsoon predictability at different timescales will likely lead to improved forecasts. Several studies have reported the multitimescale changes in predictability of the summer monsoon, from synoptic to interannual timescales. Besides, the relationship between the EASM or the SASM and El Niño-Southern Oscillation (ENSO) has also been explored, but with a focus on seasonal and interannual

timescales. For example, Ai *et al*. (2017) investigated the predictability limit of EASM indices on a synoptic timescale using the nonlinear local Lyapunov exponent method proposed by Ding and Li (2007, 2009) and demonstrated that EASM indices defined by zonal wind shear tend to be more predictive than those defined by sea-level pressure and meridional wind shear. Consequently, the monsoon index used in this study is based on zonal wind. The predictability of the monthly and seasonal-scale circulation and rainfall of the EASM and the SASM have also been examined using numerical simulations. Wang *et al*. (2004) found that nearly all atmospheric general circulation models perform poorly in simulating circulation and precipitation anomalies over the monsoon area at the monthly scale. Lee *et al*. (2010) investigated the potential ability of two climate forecast models to predict EASM precipitation and circulation one or two seasons in advance. Variability in the seasonal predictability of the summer monsoon has also been investigated (e.g., Wang *et al.,* 2005; Zhou and Zou, 2010; Yang *et al.,* 2012; Seo *et al.,* 2015; Wu and Yu, 2016), revealing that ENSO is the primary indicator of the seasonal predictability of the summer monsoon. The relationship between the EASM (SASM) and ENSO at interannual timescales has been studied extensively, demonstrating that the sea surface temperature (SST) heating center and phases of ENSO have varying effects on the monsoon system (Parthasarathy and Pant, 1985; Huang and Wu, 1989; Chen, 2002; Wu *et al.,* 2003). Whether the interdecadal relationship between the EASM (SASM) and ENSO is an important indicator of monsoon predictability remains an open question. The effects of ENSO events on the relationship between the EASM (SASM) and ENSO at interdecadal timescales also remain poorly known. These uncertainties are the primary motivation of the present study.

Here, we compare interdecadal changes in the predictability of two monsoon systems and investigate the potential effects of the ENSO-Monsoon relationship on predictability at interdecadal timescale. The reminder of this article is organized as follows. The data, indices and methods used are described in Section 2. Section 3 compares the interdecadal changes in predictability of EASM and SASM. A discussion and conclusion are provided in Section 4.

2 | DATA AND METHODS

2.1 | Reanalysis data

The SST dataset used in this study is the Extended Reconstructed SST version 3b (ERSSTv3b) dataset from the National Oceanic and Atmospheric Administration with a 2° × 2° horizontal grid resolution and covering the period 1948–2017 (Smith *et al.,* 2008). Daily mean atmospheric fields were taken from the National Centers for Environmental Prediction (NCEP1) reanalysis data, with a horizontal resolution of 2.5° × 2.5° for the period 1948–2017 (Kalnay *et al.,* 1996; Kistler *et al.,* 2001). Monthly precipitation data were obtained from the Climate Prediction Center Merged Analysis of Precipitation dataset (1979–2017) and used to examine the mechanism of the ENSO-Monsoon relationship in this paper. The climatology is derived from the whole period of each dataset.

2.2 | Indices

The Niño 3.4 index is defined as the area-average of monthly sea surface temperature anomaly (SSTA) in the region (5°S–5°N, 150°–90°W) and is often used to explore the relationship between the summer monsoon and ENSO. The Niño 3 index and the El Niño Modoki index (EMI) are similarly used to investigate two types of ENSO events with heating centers located in the eastern and central Pacific, respectively. The Niño 3 index is the area-average of monthly SSTA in the region (5°S–5°N, 170°–120°W). The EMI (Ashok *et al.,* 2007) is defined as

$$\mathrm{EMI} = [\mathrm{SSTA}]_{\mathrm{A}} - 0.5 \times [\mathrm{SSTA}]_{\mathrm{B}} - 0.5 \times [\mathrm{SSTA}]_{\mathrm{C}}, \quad (1)$$

where [] represents the area-averaged SSTA over the central Pacific (A; 10°S–10°N, 165°E–140°W), the eastern Pacific (B; 15°S–5°N, 70–110°W), and the western Pacific (C; 10°S–20°N, 125–145°E).

Wang and Fan (1999) used the area-averaged 850-hPa zonal wind (U850) over (5°–15°N, 90°–130°E) minus the area-averaged U850 over (22.5°–32.5°N, 110°–140°E) during June–August (JJA) as the EASM index:

$$\begin{aligned}\mathrm{EASM} = {} & \mathrm{U}_{850}\left(5^{\circ} - 15^{\circ}\mathrm{N}, 90^{\circ} - 130^{\circ}\mathrm{E}\right) \\ & - \mathrm{U}_{850}\left(22.5^{\circ} - 32.5^{\circ}\mathrm{N}, 110^{\circ} - 140^{\circ}\mathrm{E}\right). \quad (2)\end{aligned}$$

The SASM index using the area-averaged 850-hPa zonal wind (U850) minus the area-averaged 200-hPa zonal wind (U200) over the monsoon region (0°–20°N, 40°–110°E) from June to September (Webster and Yang, 1992) is defined as

$$\mathrm{SASM} = \mathrm{U}_{850} - \mathrm{U}_{200}\left(0^{\circ} - 20^{\circ}\mathrm{N}, 40^{\circ} - 110^{\circ}\mathrm{E}\right). \quad (3)$$

2.3 | Signal-to-noise ratio method

The signal-to-noise ratio (SNR) method has been widely used to investigate atmospheric predictability (Trenberth, 1984, 1985; Goswami, 2004). This method estimates atmospheric predictability by quantifying the relative contributions of the predictable climate signal and the unpredictable climate noise:

$$\mathrm{SNR} = \frac{\mathrm{Var(signal)} + \mathrm{Var(noise)}}{\mathrm{Var(noise)}}, \quad (4)$$

where Var(signal) represents the variance of interannual variability, and Var(noise) is the variance of the intra-annual (seasonal) variability.

One limitation of the SNR method is that only one value can be calculated from a time series to represent the potential predictability over a given period. We chose an 11-year sliding window to investigate interdecadal changes in the EASM and the SASM. In addition, the signal and noise of monsoon predictability can be separated using the SNR method to analyze their respective effects on the predictability.

3 | RESULTS

The SNR method was used to calculate potential predictability from 1948 to 2017, using an 11-year window. The interdecadal changes in EASM and SASM predictability are shown in Figure 1a. The EASM and SASM predictabilities are inversely correlated. The SASM predictability is higher than that of EASM before the 1980s, with EASM predictabilities below 8 and SASM predictabilities in the range 10–16. After this time, the SASM predictability decreases to around 8 and the EASM predictability rises to between 16 and 22 during 1977–2000. The SASM predictability then increases to above that of EASM during the 2000s.

The interdecadal monsoon signals (Figure 1b) follow the trends in predictability shown in Figure 1a. However, the EASM and SASM noise patterns differ from the signal and predictability patterns (Figure 1c), with the EASM noise (~0.4) being slightly larger than the SASM noise (0.1–0.2), which may contribute to the complexity of predicting EASM.

To examine whether the signal or the noise is the primary contributor to predictability, we calculated the correlation coefficient between the predictability in EASM and SASM, as well as their respective signals and noise. The correlation coefficient between predictability and signal for the EASM is slightly lower than that for the SASM (0.996 and 0.786, respectively; significant at the 99% confidence level). However, neither the EASM nor SASM noise is significantly correlated with predictability. Thus, the interdecadal change in monsoon predictability is correlated primarily with monsoon signal, whereas there is no significant correlation with noise.

Previous studies have revealed that ENSO is a primary contributor to the predictability of the summer monsoon. The physical mechanisms through which ENSO is related to the summer monsoon have been investigated (Nigam, 1994; Goswami, 1998; Wu *et al.,* 2012; Li *et al.,* 2018), showing that ENSO affects the SASM in developing summer and the EASM in the decayed year. The Niño 3.4 index was chosen to represent ENSO to investigate its correlation with the two summer monsoons (Figure 2). The Niño 3.4 and the SASM are significantly negatively correlated before the 1980s, whereas the positive relationship between the Niño 3.4 and the EASM becomes significant after the 1980s. Overall, EASM and SASM show opposite relationships with ENSO;

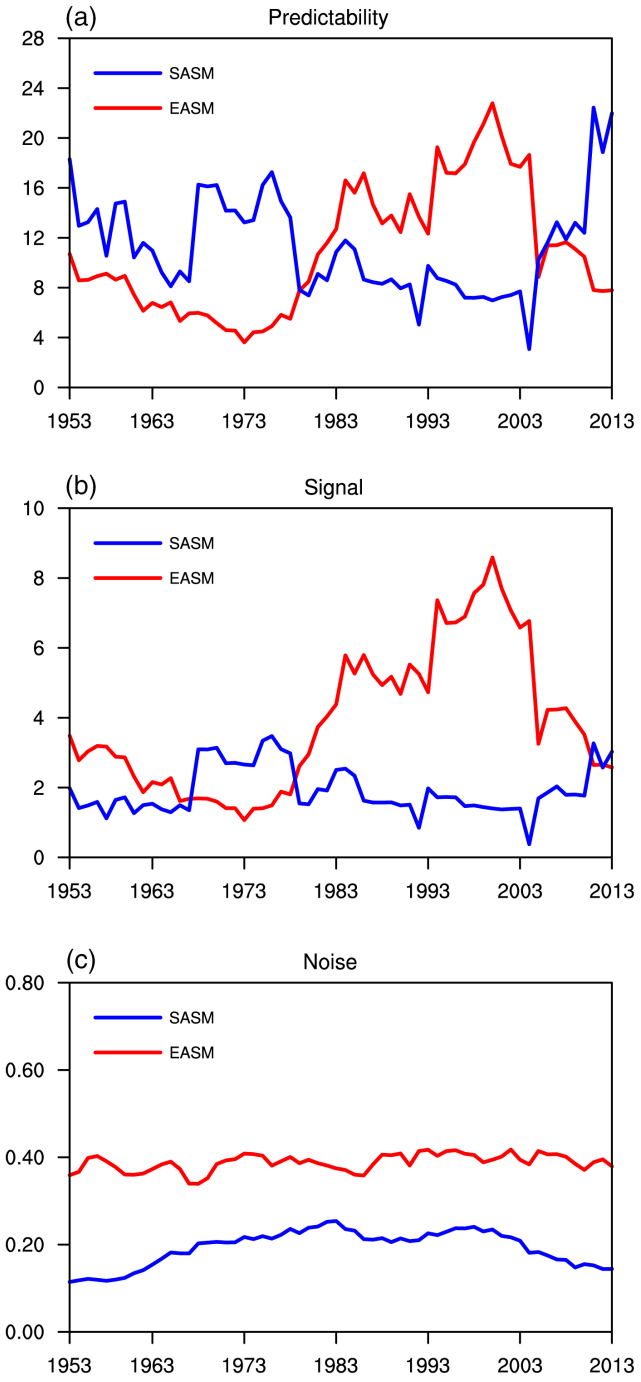

FIGURE 1 (a) Interdecadal change in the potential predictability of the EASM and the SASM from 1948 to 2017 using an 11-year sliding window, where red lines indicate the EASM and blue lines indicate the SASM. (b) and (c) Same as (a) but for signal and noise

that is, ENSO may contribute to SASM (EASM) before (after) the 1980s. Combined with the monsoon predictability (see Figure 1a), interdecadal changes in the relationship between ENSO and the summer monsoons are well correlated with predictability (Figure 2). During the period in which ENSO is significantly correlated with the EASM, predictability is high, as is the case with the SASM. Thus, interdecadal changes in the relationships between ENSO and the summer monsoon systems lead to interdecadal changes in EASM and SASM predictability.

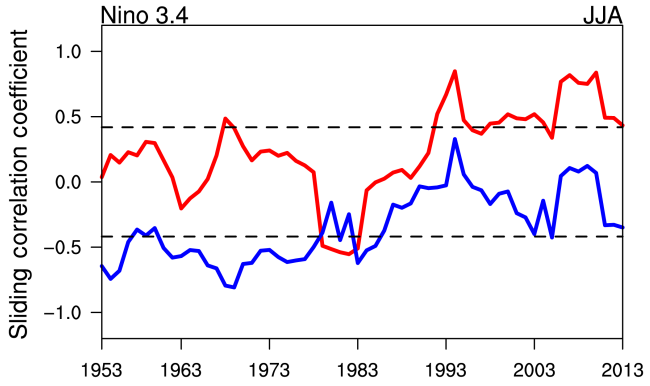

FIGURE 2 The 11-year sliding correlation coefficient between the EASM (red line) or the SASM (blue line) and the Niño 3.4 index. The dashed lines indicate the 95% confidence level

Whether these interdecadal relationships are caused by interdecadal variations in ENSO type warrants further investigation. Thus, due to the turning points of predictability and correlation coefficient occuring in Figures 1a and 2, SST anomalies related to El Niño events are divided into two preiods, 1948–1976 and 1977–2000, and shown in Figures 3a and b. The identification of El Niño events was based on the winter (December-February) Niño 3.4 index. Following the method of Yoon and Yeh (2010), events were identified for the composite analysis when the normalized index was greater than 0.5. El Niño events were identified in 1951, 1953, 1957, 1958, 1963, 1965, 1968, 1969, 1972, and 1976 during the period 1948–1976 and in 1997, 1979, 1982, 1986, 1987, 1990, 1991, 1994, and 1997 during the period 1977–2000. A composite analysis of SST anomalies shows that the location of the ENSO heating center varies on an interdecadal timescale, with SST anomalies being located primarily in the central Pacific during 1948–1976 and in the eastern Pacific during 1977–2000.

To examine whether the location of the ENSO heating center affects the summer monsoon systems, the Niño 3 index (EMI) is used to represent the ENSO heating center, which locates in the eastern (central) Pacific. The 850-hPa horizontal winds and precipitation anomalies were regressed onto the Niño 3 index (EMI) for June–August during ENSO developing and decaying years. As shown in Figures 4a and b, different ENSO heating centers lead to different wind fields and precipitation in the tropics during the summer of ENSO developing years. Compared to ENSO events with its heating center in the eastern Pacific, the ENSO events with heating centers in the central Pacific will cause more precipitation in the northwestern Pacific and less precipitation in the maritime continent and the Indian subcontinent. Precipitation anomalies cause unequal changes in latent heat release, leading to changes in the wind field. With this kind of heating, cross-scale air flow in the southern Indian Ocean is enhanced and exhibits anomalous cyclonic changes between 60° and 120°E, further affects the onset and development of the SASM. Weak precipitation anomalies caused

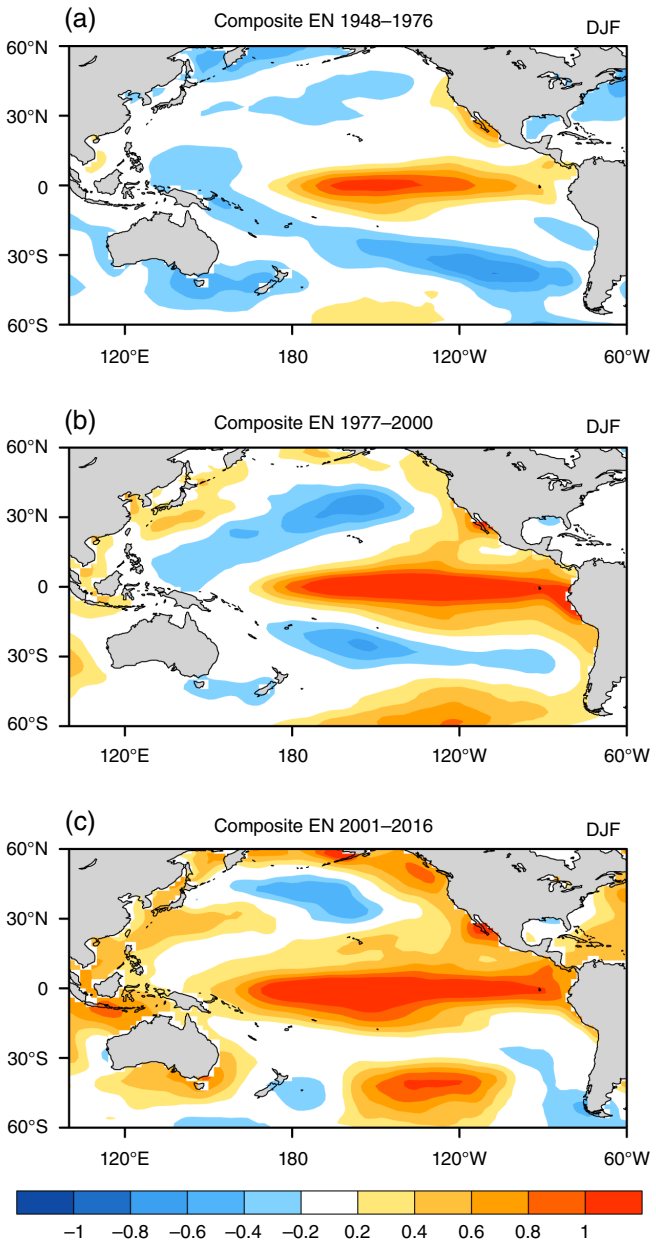

FIGURE 3 (a) Composite anomalies of SST over the tropical Pacific Ocean during winter December-February (DJF) for selected El Niño events (EN) during 1948–1976. (b) and (c) Same as (a) but for 1997–2000 and 2001–2016, respectively. El Niño events were selected for composite analysis when the normalized Niño 3.4 index was greater than 0.5

by ENSO events with heating centers in the eastern Pacific are unable to stimulate such changes in the wind field, leading to negligible impacts on the SASM. The Indian subcontinent is more arid during El Niño events than during normal years because of the downward branch of the Walker circulation. Thus, ENSO events with heating centers in the central Pacific, compared with those in the eastern Pacific, have more noticeable impacts on the SASM and lead to less precipitation over the Indian subcontinent. At the same time, warm SST anomalies coupled with heating centers in the central Pacific may enhance convection and trigger an anomalous cyclone in the lower troposphere closer to the Indian Ocean via the Gill–Matsuno mechanism, compared with the

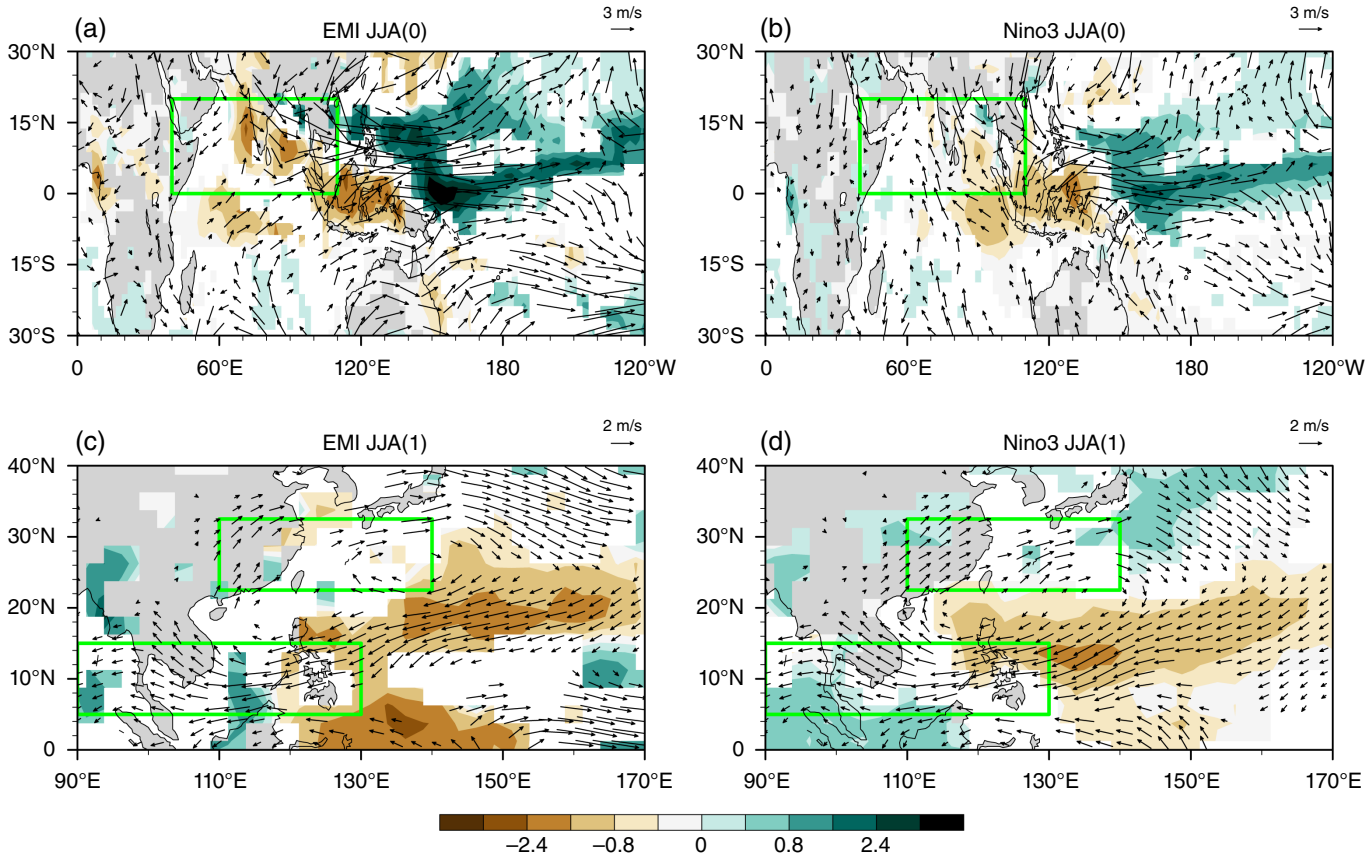

FIGURE 4 (a) Regression of 850-hPa horizontal wind (vectors) and precipitation (shading) anomalies onto (a) the EMI and (b) the Niño 3 index for summer (JJA) during ENSO developing years. (c), (d) As in (a) and (b) but for ENSO decaying years, respectively. Green rectangle in (a) and (b) denotes the region of the SASM (40°–110°E, 0°–20°N), and those in (c) and (d) denote the two regions of the EASM (90°–130°E, 5°–15°N; 110°–140°E, 22.5°–32.5°N). All shown coefficients are statistically significant at a 90% confidence level

case of ENSO events with heating centers in the eastern Pacific (Matsuno, 1966; Gill, 1980).

Wu *et al*. (2017a, 2017b) revealed that by maintaining the western North Pacific anomalous anticyclone (WNPAC), ENSO affects EASM in subsequent years. Therefore, the location of the WNPAC plays a key role in the EASM. In Figure 4c, the location of the WNPAC center caused by ENSO events with a heating center in the central Pacific is more easterly and northerly (140°E, 28°N), whereas the WNPAC center caused by ENSO events with a heating center in the eastern Pacific is located around (135°E, 20°N), near East Asia, and has a greater influence on the EASM (Figure 4d).

Figure 5 shows the average correlation coefficients between the wind fields (area defined by the monsoon index) and the Niño 3 index (EMI). During ENSO developing years, ENSO events with central-Pacific heating centers, as indicated by the EMI, show a stronger relationship with the SASM than for ENSO events with heating centers in the eastern Pacific (average correlation coefficients of 0.15 and 0.03, respectively). A weaker relationship with EASM is found for ENSO events with heating centers in the central Pacific during ENSO decaying years (an average correlation coefficient of 0.31) than for ENSO events with heating centers in the eastern Pacific (an average correlation coefficient of 0.93). These results are consistent with those shown in Figure 4. Thus, ENSO events with heating centers in the central Pacific have a significant effect on the SASM, whereas those with heating centers in the eastern Pacific have similar effects on the EASM. The location of the ENSO heating center modulates the interdecadal changes in the interannual relationship between ENSO and these monsoon systems.

4 | CONCLUSION AND DISCUSSION

The SNR method was used to analyze interdecadal changes in the predictability of the EASM and the SASM from 1948 to 2017 using reanalysis data. Results suggest that variations in SASM predictability are out of phase with those in EASM predictability. The SASM predictability is higher than EASM predictability before the 1980s, and lower during 1977–2000. Here we reveal that monsoon predictability is affected by ENSO and that the location of the ENSO heating center varies on an interdecadal timescale, which causes an interdecadal change in the ENSO-monsoon relationship. Before 1976, SASM predictability was higher than EASM predictability because the heating centers of ENSO events were in the central Pacific. Precipitation fields generated by

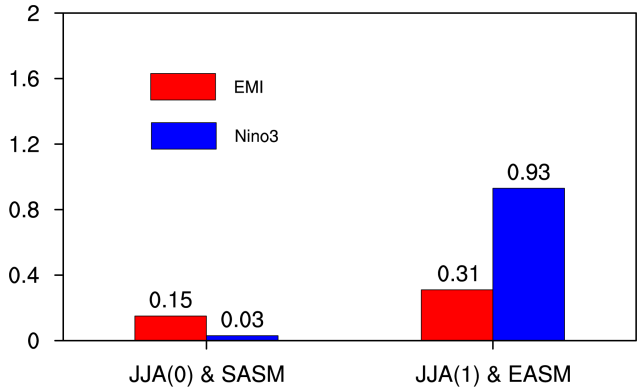

FIGURE 5 Regional average of the correlation coefficient between 850-hPa horizontal winds and the ENSO index (The regions from the green rectangles in Figure 4 represent SASM/Figures 4a,b and EASM/Figures 4c, d areas defined by the monsoon index). Red bars represent the correlation coefficient of winds and the EMI and blue bars represent those for the Niño 3 index

this type of ENSO excite wind anomalies that facilitate SASM onset and maintenance. From 1977 to 2000, the ENSO heating center was located primarily in the eastern Pacific and showed a stronger relationship with EASM in subsequent years due to the location of the WNPAC.

The Pacific decadal oscillation (PDO) modulates the interannual relationships between monsoon systems, and ENSO has been revealed in several studies (e.g., Zhu and Yang, 2003; Yoon and Yeh, 2010). Krishnamurthy and Krishnamurthy (2014) reported that the phase of the PDO may lead to better long-term predictions of seasonal monsoon rainfall and the impacts of ENSO on monsoons. Several studies have found that the PDO influences the type of ENSO. For example, Lin *et al*. (2018) pointed out that positive SST anomalies during El Niño events in the equatorial eastern Pacific are much stronger during positive PDO phases than during negative phases. Feng *et al*. (2014) found that El Niño decays slowly (rapidly) during positive (negative) PDO phases. As shown in Figure 3a and b, warm SST anomalies were located in the central Pacific for the time period from 1948 to 1976, which is correspond with the PDO negative phase, as warm SST anomalies in eastern Pacific when PDO in positive phase for 1977–2000. In addition, the PDO transfers to negative phase in recent years, and warm SST anomalies located in the central Pacific even with increased ENSO amplitudes during 2001–2016 (see Figure 3c). Thus, the PDO may be the primary contributor to interdecadal changes in the location of the ENSO heating center. However, the underlying physical processes should be explored in future work, which is also helpful for us to deepen the independence and connection between EASM and SASM.

To aid the development of seamless multiscale weather forecasts and our understanding of monsoon predictability, we investigated interdecadal changes in the EASM and the SASM. Such a comparison of the EASM and the SASM implies us that EASM (SASM) is more likely be predicted with the ENSO heating center in eastern (central) Pacific. Thus, this research enhances the understanding of predictability changes in the monsoon season, but also providing a complete framework for the monsoon prediction. Nonetheless, future work should eventually incorporate these findings into monsoon predictability over broad timescales.

ACKNOWLEDGEMENTS

This research was jointly supported by the 973 project of China (2016YFA0601801), the National Program on Global Change and Air-Sea Interaction (GASI-IPOVAI-03, GASI-IPOVAI-06), and the National Key Technology Research and Development Program of the Ministry of Science and Technology of China (2015BAC03B07).

ORCID

Baosheng Li https://orcid.org/0000-0002-3469-5192

REFERENCES

Ai, S., Chen, Q., Li, J., Ding, R. and Zhong, Q. (2017) Baseline predictability of daily East Asian summer monsoon circulation indices. *Asia-Pacific Journal of Atmospheric Sciences*, 53, 243–256.

Ashok, K., Behera, S.K., Rao, S.A., Weng, H. and Yamagata, T. (2007) El Niño Modoki and its possible teleconnection. *Journal of Geophysical Research–Oceans*, V112, C11007. https://doi.org/10.1029/2006JC003798.

Chang, C.P., Ting, I., Lau, N.C., Johnson, R.H., Wang, B. and Yasunari, T. (2011) *The Global Monsoon System: Research and Forecast. 2nd ed. World Scientific Series on Asia-Pacific Weather and Climate*, Vol. 5. Singapore: World Scientific, 590 pp.

Chen, W. (2002) Impacts of El Niño and La Niña on the cycle of the East Asian winter and summer monsoon. *Chinese Journal of Atmospheric Sciences*, 26, 595–610.

Ding, Y.H. and Chan, J.C.L. (2005) The East Asian summer monsoon: an overview. *Meteorology and Atmospheric Physics*, 89, 117–142. https://doi.org/10.1007/s00703-005-0125-z.

Ding, R.Q. and Li, J.P. (2007) Nonlinear finite-time Lyapunov exponent and predictability. *Physics Letters A*, 364, 396–400.

Ding, R.Q. and Li, J.P. (2009) Application of nonlinear error growth dynamics in studies of atmospheric predictability. *Acta Meteorologica Sinica*, 67, 241–249.

Feng, J., Wang, L. and Chen, W. (2014) How does the East Asian summer monsoon behave in the decaying phase of El Niño during different PDO phases? *Journal of Climate*, 27, 2682–2698.

Gill, A.E. (1980) Some simple solutions for heat-induced tropical circulation. *Quarterly Journal of the Royal Meteorological Society*, 106, 447–462. https://doi.org/10.1002/qj.49710644905.

Goswami, B.N. (1998) Interannual variations of Indian summer monsoon in a GCM: external conditions versus internal feedbacks. *Journal of Climate*, 11, 501–522.

Goswami, B. (2004) Inter-decadal change in potential predictability of the Indian summer monsoon. *Geophysical Research Letters*, 31, 371–375.

Huang, R.H. and Wu, Y.F. (1989) The influence of ENSO on the summer climate change in China and its mechanism. *Advances in Atmospheric Sciences*, 6, 21–32.

Kalnay, E., Kanamitsu, M., Kistler, R., Collins, W., Deaven, D., Gandin, L., Iredell, M., Saha, S., White, G., Woollen, J., Zhu, Y., Leetmaa, A., Reynolds, R., Chelliah, M., Ebisuzaki, W., Higgins, W., Janowiak, J., Mo, K.C., Ropelewski, C., Wang, J., Jenne, R. and Joseph, D. (1996) The NCEP/NCAR 40-year reanalysis project. *Bulletin of the American Meteorological Society*, 77, 437–471.

Kistler, R., Collins, W., Saha, S., White, G., Woollen, J., Kalnay, E., Chelliah, M., Ebisuzaki, W., Kanamitsu, M., Kousky, V., van den Dool, H., Jenne, R. and Fiorino, M. (2001) The NCEP-NCAR 50-year reanalysis: monthly means CD-ROM and documentation. *Bulletin of the American Meteorological Society*, 82, 247–267.

Krishnamurthy, L. and Krishnamurthy, V. (2014) Influence of PDO on south Asian summer monsoon and monsoon-ENSO relation. *Climate Dynamics*, 42, 2397–2410.

Lau, K.M. and Weng, H. (2001) Coherent modes of global SST and summer rainfall over China: an assessment of the regional impacts of the 1997-98 El Niño. *Journal of Climate*, 14, 1294–1308.

Lee, S.S., Lee, J.Y., Ha, K.J., Wang, B. and Schemm, J.K.E. (2010) Deficiencies and possibilities for long-lead coupled climate prediction of the Western North Pacific-east Asian summer monsoon. *Climate Dynamics*, 36, 1173–1188. https://doi.org/10.1007/s00382-010-0832-0.

Li, J.P. and Chou, J.F. (1997) Existence of the atmosphere attractor. *Science in China*, 40(2), 215–220.

Li, B.S., Ding, R.Q., Li, J., Xu, Y.D. and Li, J. (2018) Asymmetric response of predictability of east Asian summer monsoon to ENSO. *SOLA*, 14, 52–56. https://doi.org/10.2151/sola.2018-009.

Lin, R., Zheng, F. and Dong, X. (2018) ENSO frequency asymmetry and the Pacific decadal oscillation in observations and 19 CMIP5 models. *Advances in Atmospheric Sciences*, 35, 495–506.

Matsuno, T. (1966) Quasi-geostrophic motions in the equatorial area. *Journal of the Meteorological Society of Japan*, 44, 25–43.

Nigam, S. (1994) On the dynamical basis for the Asian monsoon rainfall-El Niño relationship. *Journal of Climate*, 7, 1750–1771.

Parthasarathy, B. and Pant, G.B. (1985) Seasonal relationship between Indian summer monsoon rainfall and southern oscillation. *Journal of Climatology*, 5, 369–378.

Seo, K.H., Son, J.H., Lee, J.Y. and Park, H.S. (2015) Northern east Asian monsoon precipitation revealed by air mass variability and its prediction. *Journal of Climate*, 28, 6221–6233. https://doi.org/10.1175/JCLI-D-14-00526.1.

Smith, T.M., Reynolds, R.W., Peterson, T.C. and Lawrimore, J. (2008) Improvements to NOAA's historical merged land-ocean surface temperature analysis (1880-2006). *Journal of Climate*, 21, 2283–2296.

Trenberth, K.E. (1984) Signal versus noise in the southern oscillation. *Monthly Weather Review*, 112, 326–332.

Trenberth, K.E. (1985) Potential predictability of geopotential heights over the southern hemisphere. *Monthly Weather Review*, 113, 54–64.

Wang, B. and Fan, Z. (1999) Choice of South Asian summer monsoon indices. *Bulletin of the American Meteorological Society*, 80, 629–638.

Wang, B., Kang, I.S. and Lee, J.Y. (2004) Ensemble simulations of Asian-Australian monsoon variability by 11 AGCMs. *Journal of Climate*, 17, 803–818.

Wang, B., Ding, Q., Fu, X., Kang, I.S., Jin, K., Shukla, J. and Doblas-Reyes, F. (2005) Fundamental challenge in simulation and prediction of summer monsoon rainfall. *Geophysical Research Letters*, 32, L15711. https://doi.org/10.1029/2005GL022734.

Webster, P.J. and Yang, S. (1992) Monsoon and ENSO: selectively interactive systems. *Quarterly Journal of the Royal Meteorological Society*, 118, 877–926.

Webster, P.J., Magaña, V.O., Palmer, T.N., Shukla, J., Tomas, R.A., Yanai, M. and Yasunari, T. (1998) Monsoons: processes, predictability, and the prospects for prediction. *Journal of Geophysical Research*, 103(C7), 14451–14510.

Wu, Z.W. and Yu, L. (2016) Seasonal prediction of the East Asian summer monsoon with a Partial-Least Square model. *Climate Dynamics*, 46, 3067–3078.

Wu, R.G., Hu, Z.Z. and Kirtman, B.P. (2003) Evolution of ENSO-related rainfall anomalies in East Asia. *Journal of Climate*, 16, 3742–3758.

Wu, Z.W., Li, J.P., He, J.H. and Jiang, Z.H. (2006) Occurrence of droughts and floods during the normal monsoons in the mid- and lower-reaches of the Yangtze River. *Geophysical Research Letters*, 33, L05813.

Wu, Z.W., Wang, B., Li, J.P. and Jin, F.F. (2009) An empirical seasonal prediction model of the east Asian summer monsoon using ENSO and NAO. *Journal of Geophysical Research*, 114, D18120.

Wu, Z.W., Li, J., Jiang, Z., He, J. and Zhu, X. (2012) Possible effects of the North Atlantic oscillation on the strengthening relationship between the East Asian summer monsoon and ENSO. *International Journal of Climatology*, 32, 794–800.

Wu, B., Zhou, T. and Li, T. (2017a) Atmospheric dynamic and thermodynamic processes driving the western North Pacific anomalous anticyclone during El Niño. Part I: maintenance mechanisms. *Journal of Climate*, 30(23), 9621–9635. https://doi.org/10.1175/JCLI-D-16-0489.1.

Wu, B., Zhou, T. and Li, T. (2017b) Atmospheric dynamic and thermodynamic processes driving the western North Pacific anomalous anticyclone during El Niño. Part II: formation processes. *Journal of Climate*, 30(23), 9637–9650. https://doi.org/10.1175/JCLI-D-16-0495.1.

Yang, D.J., Tang, Y.M., Zhang, Y.C. and Yang, X.Q. (2012) Information-based potential predictability of the Asian summer monsoon in a coupled model. *Journal of Geophysical Research*, 117, D03119. https://doi.org/10.1029/2011JD016775.

Yoon, J. and Yeh, S.W. (2010) Influence of the Pacific decadal oscillation on the relationship between El Niño and the northeast Asian summer monsoon. *Journal of Climate*, 23, 4525–4537. https://doi.org/10.1175/2010JCLI3352.1.

Zhou, T.J. and Zou, L.W. (2010) Understanding the predictability of East Asian summer monsoon from the reproduction of land-sea thermal contrast change in AMIP-type simulation. *Journal of Climate*, 23, 6009–6026. https://doi.org/10.1175/2010JCLI3546.1.

Zhu, Y.M. and Yang, X.Q. (2003) Relationship between Pacific decadal oscillation and climate variabilities in China. *Acta Meteorologica Sinica*, 61, 641–654.

How to cite this article: Li B, Ding R, Qin J, Zhou L, Hu S, Li J. Interdecadal changes in potential predictability of the summer monsoon in East Asia and South Asia. *Atmos Sci Lett*. 2019;20:e890. https://doi.org/10.1002/asl.890